

MOL #83964

**Adiponectin ameliorates iron-overload cardiomyopathy through the
PPAR α -PGC-1-dependent signaling pathway**

Heng Lin, Wei-Shiung Lian, Hsi-Hsien Chen, Pei-Fang Lai, and Ching-Feng Cheng

Department of Medical Research, Tzu Chi General Hospital and Department of Pediatrics, Tzu Chi University, Hualien, Taiwan (W.-S.L., C.-F.C.); Institute of Biomedical Sciences, Academia Sinica, Taipei, Taiwan (W.-S.L., C.-F.C.); Department of Physiology, School of Medicine, College of Medicine, Taipei Medical University, Taipei, Taiwan (H.L.); Department of Internal Medicine, School of Medicine, College of Medicine, Taipei Medical University, Taipei, Taiwan (H.-H.C.); Division of Nephrology, Department of Internal Medicine, Taipei Medical University Hospital, Taipei, Taiwan (H.-H.C.); PhD Program in Pharmacology and Toxicology, Tzu Chi University, Hualien, Taiwan (P.-F.L.); Department of Emergency Medicine, Tzu Chi General Hospital, Hualien, Taiwan (P.-F.L.)

MOL #83964

Running title: Adiponectin attenuates iron-overload cardiomyopathy

Correspondence : Dr. Ching-Feng Cheng. Department of Medical Research, Tzu Chi

General Hospital and Department of Pediatrics, Tzu Chi University, Hualien, Taiwan.

Address: 707, Chung-Yang Road, Section 3, Hualien City, Taiwan; Telephone:

886-3-8561825, ext:5629; Fax: 886-3-8567043; e-mail: chengcf@mail.tcu.edu.tw

Number of:

Text pages: 44

Table: 1

Figure: 6

Reference: 47.

Words in Abstract: 240

Words in Introduction: 421

Words in Discussion: 1112

Abbreviations: PPAR, peroxisome proliferator-activated receptor; HO-1, heme oxygenase-1; PGC1, Peroxisome proliferator-activated receptor gamma coactivator-1; ChIP, chromatin immune-precipitation; AAV, adeno-associated virus; LV, left ventricle; MOI, multiplicities of infection; HPGK, human phosphoglycerate kinase.

ABSTRACT

Adiponectin is a circulating adipose-derived cytokine that may act as an anti-oxidative and anti-inflammatory protein. Although adiponectin has been reported to exert cytoprotective effects in acute cardiac diseases, its effects on chronic heart failure are less clear. Therefore, we aimed to investigate whether adiponectin would have a beneficial effect in iron-induced chronic heart failure and to elucidate its regulation in cardiomyocytes. Mice were first treated with iron dextran for 4 weeks to induce iron-overload cardiomyopathy. They exhibited decreased survival with impaired left ventricle contractility and decreased serum adiponectin levels. *In vivo* cardiac adiponectin gene (*ADIPOQ*) over-expression with AAV-*ADIPOQ* ameliorated cardiac iron deposition and restored cardiac function in iron-overloaded mice. In addition, AAV-*ADIPOQ* treated iron-overload mice had lower expression of inflammatory markers, including myeloperoxidase activity, MCP-1, TNF- α , IL-6 and ICAM-1, than iron overloaded mice not treated with AAV-*ADIPOQ*. Our *in vitro* study showed that adiponectin induced heme oxygenase-1 (HO-1) expression through the PPAR α -HO-1 signaling pathway. Furthermore, the adiponectin-mediated beneficial effects were PPAR α -dependent as the adiponectin-mediated attenuation of iron deposition was abolished in PPAR α -knockout mice. Finally, PPAR α -HO-1 signaling involved PPAR α and PGC-1 binding and nuclear translocation, and their

MOL #83964

levels were increased by adiponectin therapy. Together, these findings suggest that adiponectin acts as an anti-inflammatory signaling molecule and induces the expression of HO-1 through the PPAR α -PGC-1 complex-dependent pathway in cardiomyocytes, resulting in the attenuation of iron-induced cardiomyopathy. Using adiponectin for adjuvant therapies in iron-overload cardiac dysfunction may be an option in the future.

Introduction

Recent advances in adipose biology have provided convincing evidence that adipose tissue can function as an endocrine organ by secreting adipocytokines that influence metabolism in peripheral tissue. Adiponectin is a circulating adipose-derived cytokine that may act as an anti-oxidative and anti-inflammatory protein and suppress cytokine production in activated macrophages (Zoccali et al., 2002; Cheng et al., 2012; Tian et al., 2012). Previous studies have demonstrated that adiponectin attenuates cardiac hypertrophy in response to pressure overload (Shibata et al., 2004) and reduces atherosclerosis through its vascular anti-inflammatory effects in the cardiovascular system (Hopkins et al., 2007; Hajer et al., 2008; Maury and Brichard, 2010; Vaiopoulos et al., 2012).

Iron can form highly reactive oxygen free radicals, which cause peroxidation of membrane lipids and oxidative damage to cellular proteins (Crowe and Bartfay, 2002), and iron-overload cardiomyopathy is commonly seen in patients who need long-term blood transfusions, such as patients with thalassemia major or hereditary hemochromatosis. Although iron chelation therapy is widely used to treat iron-overload conditions, recent data have shown that iron-overload cardiomyopathy is the primary determinant of cardiac complications and survival in these patients

(Fraga and Oteiza, 2002).

Lin et al. demonstrated that adiponectin exerts its protective effects against iron-induced liver injury through PPAR α -dependent HO-1 induction (Lin et al., 2010). Cheng et al. demonstrated a similar mechanism in which adiponectin exerts a protective effect against acute renal ischemia-reperfusion (I/R) injury through the prostacyclin-PPAR α -HO-1 signaling pathway (Cheng et al., 2012). These results suggest that adiponectin protects against *in vivo* tissue inflammation and oxidative stress through PPAR α signaling. Recently, Gabrielsen et al. reported that iron levels in adipocytes can regulate the levels of adiponectin transcription and serum protein and that decreasing tissue iron stores can decrease ferritin and increase adiponectin (Gabrielsen et al., 2012). They suggested that adipocytes play a role in modulating metabolism and diabetic risks through adiponectin in response to iron stores. However, it is unclear whether adiponectin levels are affected by iron stores in cardiomyocytes, which are commonly observed in patients with iron-overload cardiomyopathy. In addition, since the function of adiponectin gene (ADIPOQ) has not been studied, and the possible involvement of the PPAR α -HO-1 signaling pathway in chronic cardiomyopathy is still unclear, we overexpressed ADIPOQ both *in vitro* and *in vivo* to test the effect of ADIPOQ overexpression on iron-overload-induced cardiac

MOL #83964

dysfunction. We also examined whether PPAR α and/ or PGC-1 α signaling was involved in regulation of ADIPOQ. We found that adiponectin ameliorated iron deposition in the heart through a PPAR α -PGC-1-dependent mechanism and that adiponectin can exert beneficial effects in iron-overload cardiomyopathy.

Materials and Methods

Iron loading administration and serum ELISA analysis

Male C57/B6, H129 PPAR α knockout mice, and their wild type littermates received humane care in compliance with the Principles of Laboratory Animal Care of National Society for Medical Research and the Guide for the Care and Use of Laboratory Animals prepared by the Institute of Laboratory Animal Resources (NIH publication No. 86-23, revised 1985). The study protocol was approved by the institutional ethics committee on animal research. Mice (male, body weight (bw): 25-30 gm) were randomly divided into different experimental groups. Iron dextran (Sigma-Aldrich Co. U.S.A.) was i.p. injected to one group at 10 mg/ 25 gm bw/day, 5 days/week for four weeks to create an iron loading group, as previously described (Lian et al., 2011). The mice in the control group were injected with dextrose (0.1 ml of 10%) the same time over the same period. Mouse sera were harvested for APN, IL-6, MCP-1, ICAM-1 and TNF- α via ELISA kit (Quantikine® ELISA, R&D systems, Germany) with reader (450 nm with a correction at 570 nm) used for semi-quantification.

Isolation of cardiomyocytes and cell line culture

Neonatal cardiomyocytes were isolated and cultured according to the method of Fujio et al. with some modifications (Fujio et al., 2002). Briefly, the cardiac ventricles of

MOL #83964

neonatal Wistar rats (male and female, 1-2 days old) were digested with pancreatin (1.25 mg/ml) at 37°C. Cardiomyocytes were isolated and cultured in DMEM containing 10% fetal bovine serum and 0.1 μ M bromodeoxyuridine. After 3 days, cells were incubated in serum-free medium containing transferrin (5 μ g/ml), insulin (5 μ g/ml), and 0.1 μ M bromo-deoxyuridine for 24 hours before further treatment with indicated agents. The rat H9c2 cells were acquired from ATCC and were routinely maintained in high glucose DMEM supplemented with 10% fetal bovine serum (FBS), penicillin and streptomycin.

Luciferase reporter assay and chromatin immunoprecipitation (CHIP) assay

HO-1 promoter (-1421~1400) containing a PPRE-binding sequence were cloned into pGL2-basic vectors (Promega) and transfected into H9c2 cells. Promoter-induced luciferase activity was measured as described previously (Chen et al., 2009). H9c2 cells were treated with adiponectin and fixed in 1% formaldehyde, and chromatin immunoprecipitation (ChIP) assay was performed following the manufacture's protocol (Millipore). Chromatin was immune-precipitated with PPAR α (1mg, Santa Cruz Biotechnology) antibody. Purified DNA was then detected with HO-1 promoter primers by standard polymerase chain reaction.

Preparation of ADIPOQ recombinant virus and protein production

Full-length cDNA of human ADIPOQ was constructed and transformed into BL-21 *Escherichia coli* and induced by 1 mmol/L IPTG for 20 hours. Following a standard protocol, adiponectin protein was harvested from *E. coli* when the OD600 of the *E. coli* broth reached 0.5. Then, Ni-NTA column and FPLC gel filtration column (HiLoad 16/60 superdex 2000) were added for purification. For adeno-associated virus-ADIPOQ (AAV-ADIPOQ) and adenovirus-ADIPOQ (Adv-ADIPOQ) construction, full-length ADIPOQ cDNA was respectively cloned into the pAAV8-CMV-MCS vector and a human phosphoglycerate kinase (HPGK) promoter was used to drive ADIPOQ expression. The experimental protocol has been described in detail in prior studies (Lin et al., 2002; Lin et al., 2010). The recombinant AAV-ADIPOQ (with 1×10^{12} viral particles in 50 μ l of saline) was injected into a mouse tail vein (i.v.) two weeks before the iron treatment. The Adv-HPGK and Adv-ADIPOQ were transduced to cells at different multiplicities of infection (MOI). The recombinant protein of adiponectin, used for *in vitro* study, was treated to cells in dose-dependent manners.

Tissue RNA extraction and RT-PCR

The recombinant AAV-ADIPOQ was injected into a mouse's tail vein and then tissues

MOL #83964

from heart, liver, kidney, fat tissue, and muscle were harvested 2 weeks later. Total RNA from individual tissue was extracted by Trizol reagent and homogenized with TissueRuptor (Qiagen). The cDNA from 3 µg RNA was used for reverse transcription using a High-Capacity cDNA reverse transcription kit (ABI, Life Technologies). Quantitative PCR was done using a LightCycler480 (Roche Diagnostics, Mannheim, Germany) and a detection agent PerfeCTa™ SYBR® Green FastMix™ (Quanta Biosciences, Inc.). Specific primers for ADIPOQ sense, 5'-AAGGGCTCAGGATGCTACTGTT-3', and antisense, 5'-AGTAACGTCATCTTCGGCATGA-3'; TNF-α sense, 5'-TACTGAACTTCGGGGTGATTGGTCC-3' and antisense, 5'-GGTTCTCTTCAAGGGACAAGGCTG-3'; and ICAM-1 sense, 5'-CGCAAGTCCAATTCACACTGA-3', and antisense, 5'-ATTCAGAGTCTGCTGAGAC-3 were used and GAPDH for an internal control. The relative expression ratio of ADIPOQ was calibrated with GAPDH and then compared to control group.

Western blotting and immunoprecipitation

The cell pellets were harvested by centrifugation at 250×g/5 min at 4°C and were separated into cytoplasmic and nuclear parts using a ProteoJET™ protein extraction

MOL #83964

kit (Fermentas Life Sciences). Protein concentration was determined by Bio-Rad protein assay. Equal amounts of extracted proteins were separated by SDS-PAGE electrophoresis, transferred to polyvinylidene fluoride membranes (PVDF; Millipore Corporation), and probed with primary antibodies; rabbit anti-PGC-1 (1:2000; Santa cruz), rabbit anti-PPAR α (1:1000; Santa cruz), mouse anti-adiponectin (1:1000; Abcam), rabbit anti-p-AMPK (1:1000; Cell signaling), rabbit anti-AMPK (1:1000; Cell signaling), and rabbit anti-HO-1 (1:1000; Santa cruz). Mouse anti-actin (1:100,000; Abcam), mouse anti-GAPDH (1:3000; Millipore), and rabbit anti-LaminA/C (1:3000; GeneTax) were used as internal controls. For immunoprecipitation, the total cell lysate was prepared by IP lysis buffer (Pierce biotechnology, Thermo) and follow by two to three preclearings with protein A/G agarose to ensure complete removal of endogenous Igs. The IP/WB Optima C (ImmunoCruz IP/WB Optima F, Santa Cruz) was used for IP antibody/IP matrix formation with the addition of 5 μ g of PPAR α . 500 μ g of lysate was then transferred to the specific IP matrix at 4°C on a rotator for overnight rotation. After incubation, the pellet IP matrixes were washed and boiled with 2x sample buffer for western blotting analysis.

Immuno-histochemistry for left ventricular tissue

MOL #83964

Mice hearts were perfused through the left ventricle (LV) with 4% paraformaldehyde in 0.1 M PBS. The paraffin-embedded cardiac cross sections (5 μ m) were stained with iron-specific-Prussian blue. Positive stained cells were counted using an image analysis system (Image-Pro Plus v6.0; Media Cybernetics, Inc).

Echocardiography studies

Mice were anesthetized with pentobarbital (50 mg/kg body weight, ip). The anterior chest was shaved and laid in a left decubitous position. Gel was applied on the chest wall for better scanhead-skin contact. The echocardiography system (HDI 5000, Phillips, U.S.A.) had equipped with 2D, M-mode, and pulse wave Doppler imaging. Heart rate, left-ventricle (LV) dimension in both systolic and diastolic stages and the LV fractional shortening/ejection fraction were measured.

Measurement of biochemical parameters, blood counts and MPO Activity

Complete blood counts and leukocytes classification were performed using CELL-DYN® 3700 (Abbott Park, Illinois, U.S.A.). The MPO, an indication of neutrophil infiltration into tissue, was measured as previously described (Bradley et al., 1982).

MOL #83964

Statistical Analyses

All data are expressed as the means \pm SEM or means \pm SD for blood count test.

Survival analysis was performed by Kaplan–Meier method, and between-group differences in survival rates were tested by log rank test. Between-group comparisons of the means were performed by one-way ANOVA, followed by t-tests. The Bonferroni’s correction was performed for multiple comparisons of the means.

Results

Decreased serum adiponectin levels were found in mice with iron-overload cardiomyopathy

We established mice with iron-overload cardiomyopathy as prior studies (Lian et al., 2011) and these mice showed a decreased survival rate after four weeks of iron loading (Fig. 1A). Serum adiponectin levels were significantly lower in mice after four weeks of iron supplement compared with the control group (Fig. 1B). These findings suggested that chronic iron loading attenuated serum adiponectin concentrations *in vivo*.

Cardiac ADIPOQ overexpression ameliorated iron deposition in the heart and restored normal cardiac function

To determine whether ADIPOQ replacement attenuated iron-overload cardiomyopathy, we established a stable and homogenous expression system for ADIPOQ in mouse heart with AAV8, as previously reported (Wang et al., 2005). The expression of ADIPOQ increased significantly in the heart after two weeks of i.v. injections of the AAV-ADIPOQ (Fig. 2A). Other organs, including liver, kidney, muscle, and fat tissue, also showed increased levels ADIPOQ expression (Fig. 2B). Consistent with the above results, the serum levels of adiponectin were also markedly

MOL #83964

increased in the AAV-ADIPOQ experimental group compared with the AAV-CMV-treated control group, likely due to our i.v. infusion of AAV-ADIPOQ with multiple organs expression of ADIPOQ (Fig. 2C). To further investigate the effects of adiponectin on attenuating cardiac iron deposition, we compared sections from the heart tissue in mice that were or were not treated with ADIPOQ following iron loading. ADIPOQ overexpression markedly attenuated iron accumulation in the heart of mice compared with the control group that were not treated with ADIPOQ (Fig. 2D). In addition, ADIPOQ treatment also restored normal cardiac function by increasing left ventricular fractional shorting (FS) and ameliorating left ventricular chamber dilation in iron-loaded hearts compared with the untreated iron-loaded group (Fig. 3A). Together these findings show that *in vivo* adiponectin supplementation to the heart minimized / reduced iron-overload-induced cardiomyopathy.

ADIPOQ overexpression suppressed inflammatory responses in iron-overload cardiomyopathy

Because iron loading can induce reactive oxygen species (ROS) and associated myocardial inflammation that resulting in chronic cardiac dysfunction (Oudit et al., 2003; Bartfay et al., 1999), we next investigated whether adiponectin replacement with AAV-ADIPOQ would inhibit iron-induced inflammatory responses in the heart.

MOL #83964

As seen in Figure 3B, myocardial myeloperoxidase activity, derived mainly from infiltrated neutrophils, was reduced by one-third (0.68 v.s. 0.21) in the ADIPOQ-treated group (AAV8-ADIPOQ) compared with the control group (AAV8-CMV). We also examined the cardiac inflammatory profile, including the levels of TNF- α , IL-6, MCP-1, and ICAM-1, by ELISA analysis after four weeks of iron loading. The ADIPOQ-treated group showed decreased sera levels of IL-6, MCP-1, and ICAM-1, and a very large reduction (50%) in TNF- α (Fig. 3C), and heart tissue levels of ICAM-1 and TNF- α (Fig. 3D). As can be seen in Table 1, a summary of a complete blood count analysis, lower numbers of leukocytes and lymphocytes were found in the ADIPOQ + iron-treated group compared with the group treated with iron alone.

Adiponectin induced HO-1 expression in neonatal cardiomyocytes through the PPAR α -HO-1 signaling pathway

Our previous report demonstrated that adiponectin inhibits renal I/R injury through HO-1 induction (Cheng et al., 2012). Because a PPAR α response element, PPRE, is located in the HO-1 promoter region, we examined whether adiponectin exerts its beneficial effects in iron-overload cardiomyopathy through this pathway. As seen in Figure 4A, adiponectin increased the expression of p-AMPK and HO-1. To further

examine the interactions between adiponectin and HO-1, and the translocation of PPAR α from the cytosol to the nucleus, neonatal cardiomyocytes were infected with adenovirus that contained ADIPOQ or HPGK for assessment of HO-1 induction. Our data showed that HO-1 expression (Fig. 4B) and the PPAR α nuclear translocation (Fig. 4C) can be induced by Adv-ADIPOQ in a time-dependent manner (with 100 moi virus infection). We wanted to investigate whether adiponectin-induced HO-1 expression was dependent on the translocation/binding of PPAR α to the PPRE element. We selected a PPAR binding sequence located in the HO-1 promoter (–1421 to –1400 bp) and examined whether the PPAR α protein was located in the nucleus and whether it was associated with the PPRE. To do this, we used a ChIP assay with both control and adiponectin-stimulated cells at various intervals of incubation (Fig. 4D). Adiponectin-induced association between the PPAR α and PPRE region of the HO-1 promoter, with subsequent HO-1 expression, was strongest 0.5 hours after adiponectin treatment followed by gradual attenuation (Fig. 4A and 4D). Finally, to determine the activity of adiponectin-induced PPAR α binding to the PPRE (HO-1 promoter), we transfected luciferase expression vectors (pGL2) with the HO-1 promoter containing PPRE binding sites in H9c2 cells, and infected with different amounts (50 moi or 100 moi) of adenovirus containing either ADIPOQ or HPGK. Increased luciferase activity was found in Adv-ADIPOQ infected with 100 moi but

not 50 μM (Fig. 4E). Concordantly, we found increased luciferase activity in H9c2 cells treated with 20 μg of adiponectin, but not in those infected with 10 μg (Fig. 4F). These findings suggest that adiponectin might act in a paracrine or autocrine manner to induce HO-1 expression through the PPAR α translocation pathway in order to attenuate iron deposition in the heart.

The beneficial effects of adiponectin-mediated PPAR α -HO-1 in iron-overload cardiac dysfunction were PPAR α -dependent

We next examined the adiponectin-mediated PPAR α -HO-1 signaling pathway in iron-overloaded mice to determine if the beneficial effects depended on the existence of PPAR α , or, more frequently, a redundant function among other PPARs family. To do this, PPAR α gene-deleted (PPAR $\alpha^{-/-}$) mice and their wild-type littermates were subjected to four weeks of iron loading and ADIPOQ overexpression, as described above. Figure 5 shows that the adiponectin-mediated beneficial effects were completely abolished in the PPAR $\alpha^{-/-}$ mice. PPAR $\alpha^{-/-}$ mice both with and without ADIPOQ therapy had the same levels of iron deposition in the heart. Surprisingly, higher levels of iron deposition were found in PPAR $\alpha^{-/-}$ mice than in the wild-type mice not treated with ADIPOQ. This finding suggests that PPAR α , itself, can exert a protective role against iron deposition independent of the adiponectin-mediated

pathway, confirming that adiponectin-mediated PPAR α -HO-1 beneficial effects against iron-overload cardiac dysfunction were PPAR α dependent.

Involvement of the PGC-1-PPAR α complex in the nucleus in the adiponectin-induced HO-1 expression

Because the association between the transcriptional coactivator, PGC-1, and PPAR α plays important roles in cardiac nutritional and metabolic regulation (Haemmerle et al., 2011), we wondered whether PGC-1 was also involved in the regulation of adiponectin-mediated cardiac protection. As can be seen in Figure 6A, twenty-four hours of iron loading in H9c2 cells resulted in a reduction in both cytoplasmic PGC-1 and PPAR α levels and a concomitant increase in the levels of nuclear PGC-1 and PPAR α . This finding indicated that both PGC-1 and PPAR α translocated from cytoplasmic to nuclear fractions during iron-induced stress. Adiponectin supplementation to H9c2 cells increased both the cytoplasmic and nuclear expression of PGC-1 and PPAR α , suggesting that adiponectin upregulated cytoplasmic PGC-1 and PPAR α signaling, and subsequent nuclear translocation of both components (Fig. 6B). To further confirm the interactions between PPAR α and PGC-1 during adiponectin or iron treatment, an immunoprecipitation assay was conducted with H9c2 cells. Figure 6C shows that adiponectin treatment increased the binding between

MOL #83964

PPAR α and PGC-1, and this interaction was reduced by iron loading, indicating that adiponectin exerted its cytoprotective effects against iron loading through increased binding between PPAR α and PGC-1 and their nuclear translocation.

Discussion

In this study, we first demonstrated decreased serum levels of adiponectin in our mouse model of iron-overload cardiomyopathy. In addition, ADIPOQ overexpression ameliorated cardiac iron deposition and suppressed inflammatory responses, improving left ventricular contraction in iron-overload cardiomyopathy. Moreover, our *in vitro* studies showed that the beneficial effects of adiponectin were mediated by the PPAR α -dependent HO-1 signaling pathway and required PPAR α -PGC-1 interaction. Our study elucidates the cytoprotective effects of adiponectin in iron-induced cardiac dysfunction.

Previous studies have reported that patients with aortic stenosis or diabetes mellitus-induced cardiomyopathy have low circulating levels of adiponectin and high levels of proinflammatory cytokines (Pischon et al., 2011; Baldasseroni et al., 2012; Won et al., 2012), and one epidemiological study has found an association between low serum levels of adiponectin and an increased risk of coronary artery disease (CAD) and severity of CAD in patients with metabolic syndrome (Kumada et al., 2003). Decreased adiponectin levels have also been reported in animal models of ischemia/reperfusion (I/R) injury, ventricular hypertrophy, and doxorubicin-induced cardiomyopathy (Shibata et al., 2004; Shibata et al., 2005; Konishi et al., 2011; Wang

et al., 2010). Furthermore, recent studies have found a negative correlation between the levels of serum ferritin and adiponectin (Forouhi et al., 2007; Mojiminiyi et al., 2008; Ku et al., 2009), suggesting that adipocyte iron negatively regulates ADIPOQ transcription *via* FOXO-1-mediated repression (Gabrielsen et al., 2012). These findings indicated that increased tissue iron stores are sufficient to increase serum ferritin and decrease serum adiponectin levels. Iron loading induced oxidative stress with the overexpression of proinflammatory molecules, such as IL-6, MCP-1, TNF- α , and ICAM-1, in heart or blood vasculature (Kahn et al., 2010), which leads to endothelial and cardiac dysfunction. Therefore, it is plausible that decreased levels of adiponectin could be a risk index in cardiac inflammation and associated endothelial dysfunction. In addition, because adiponectin can exert beneficial effects on atheroprotection and anti-inflammation (Hopkins et al., 2007; Zhu et al., 2008), adiponectin is an ideal index, as well as therapy molecule, for cardiovascular diseases.

Previous studies on liver energy regulation have demonstrated that adiponectin has two receptors, which have clearly different signaling pathways. AdipoR1, which is linked to the activation of the AMPK pathway, regulates the inhibition of liver glucose production and increases in fatty acid oxidation, while AdipoR2 is mainly linked to the activation of the PPAR α pathway, which stimulates energy dissipation and inhibits

inflammation and oxidative stress. AdipoR1 is abundantly expressed in muscular cells, including cardiomyocytes, whereas adipoR2 is predominantly expressed in the liver. As adiponectin circulates in serum in either the low-molecular-weight (LMW) form or the high molecular weight (HMW) form, the LMW has high binding affinity to AdipoR1 and lower binding affinity with AdipoR2, whereas the HMW has the opposite binding affinity, low to AdipoR1 and high to AdipoR2. Because the overexpressed ADIPOQ that was used in our studies was purified from *Escherichia coli*, it mostly existed in the HMW form (Cheng et al., 2012). Thus, it binds to AdipoR2 with high affinity and to adipoR1 with low affinity. The result of this study suggests that AdipoR2-PPAR α signaling might be the major pathway exerting anti-inflammatory and anti-oxidative stress effects that ameliorate iron-induced cardiac dysfunction. This study also found that these cardioprotective effects were mediated through PPAR α signaling, suggesting the existence of cross talk between adipoR1/adipoR2 signaling and the paracrine/autocrine functions of adiponectin in the heart. Recent studies have demonstrated that adiponectin production in the heart can be increased by PPAR γ , and the amount of induction is determined by coactivator combination or by the ubiquitination levels of PPAR γ or PPAR α (Genini and Catapano, 2006).

MOL #83964

PPAR α , which belongs to the PPAR family, can exhibit anti-inflammatory effects. PPAR α agonists or adenoviral-mediated PPAR α overexpression in cardiomyocytes can induce the expression of genes involved in fatty acid catabolic pathways, which involve the esterification, binding, transportation, and the β oxidation of fatty acids (Barger et al., 2000; Huss et al., 2001; Gilde et al., 2003). The activation of PPAR α has been reported to protect normal or diabetic myocardium against I/R injury through PI3-Kinase/Akt pathway (Bulhak et al., 2009). However, the constant overexpression of PPAR α in the heart with cardiac specific myosin heavy chain (α -MHC) promoter results in increased fatty acid oxidation with decreased glycolysis, which causes left ventricular dysfunction with lipotoxicity (Finck et al., 2002; Finck et al., 2003). These findings support the hypothesis that the beneficial role of PPAR α may depend on its coactivators or a different complicated regulation.

PGC-1 α , which is the transcriptional coactivator of PPARs, has recently emerged as a key player in the control of myocardial metabolism (Rowe et al., 2010). In cardiac myocytes, the activation of PGC-1 α drives a strong induction of PPAR α target genes that encode FAO enzymes (Lehman et al., 2000). PGC-1 α can also coactivate other transcription factors to stimulate mitochondrial biogenesis and enhance the expression of components of the electron transport chain (Lehman et al., 2000; Huss et al., 2002;

Huss et al., 2004). One previous study has indicated that adiponectin can inhibit cardiomyocyte apoptosis through the AMPK or APNR1-AMPK-PGC-1 pathway (Konishi et al., 2011), and our data shows that adiponectin can induce PPAR α that is associated with PGC-1 into the nucleus to inhibit inflammatory responses in iron loading. Whether the adiponectin induced beneficial effects of PPAR α -PGC-1 on iron-overload cardiac dysfunction come about as a result of PGC-1 induction of increased mitochondria activity or its induction of anti-ROS related gene expression will need to be further evaluated. One recent study by Haemmerle et al. has reported that hydrolysis of cardiac lipid droplets by adipose triglyceride lipase is required to activate PPAR-mediated PGC-1 expression (Haemmerle et al., 2011). This regulation, which specifically occurs in the heart but not in the liver, is PPAR α dependent (but not for PPAR γ). Although the exact component of this putative ligand for PPAR α is still unknown, our data suggest that PPAR α -PGC-1 signaling is essential for maintaining mitochondrial oxidative capacity and ATP generation, which is required for myocardial contractility.

In summary, adiponectin has been reported to exert beneficial effects on acute myocardial infarction and I/R injury, and our study further validated the protective role of adiponectin in chronic cardiomyopathy that was induced by iron loading.

MOL #83964

However, higher adiponectin serum levels are reported to correlate with increased mortality in patients with chronic heart failure (Beatty et al., 2012), thus raising questions on the beneficial role of adiponectin. It is likely that functional adiponectin resistance develops in patients with advanced heart failure with down regulation of adiponectin receptors (Springer et al., 2010; Khan et al., 2012). These findings indicate the importance to clearly delineate the downstream signaling and cross talk of adiponectin regulation before we can use adiponectin as a future therapeutic regimen for cardiovascular disease.

MOL #83964

Acknowledgements

We thank Ms Pei-Chi King for mouse surgery and mouse husbandry.

Authorship contributions

Participated in research design: Lin and Cheng

Conducted experiments: Lian and Chen

Contributed new reagents or analytic tools: Lai

Performed data analysis: Lin, Lian, and Cheng

Contributed to the writing of the manuscript: Lin, Lian, and Cheng

References

- Bradley PP, Priebat DA, Christensen RD and Rothstein G (1982) Measurement of cutaneous inflammation: estimation of neutrophil content with an enzyme marker. *J Invest Dermatol* **78**:206-209.
- Bartfay WJ, Butany J, Lehotay DC, Sole MJ, Hou D, Bartfay E and Liu PP (1999) A biochemical, histochemical, and electron microscopic study on the effects of iron-loading on the hearts of mice. *Cardiovasc Pathol* **8**:305-314.
- Baldasseroni S, Mannucci E, Orso F, Di Serio C, Pratesi A, Bartoli N, Marella GA, Colombi C, Foschini A, Valoti P, et al. (2012) Adiponectin in outpatients with coronary artery disease: independent predictors and relationship with heart failure. *Nutr Metab Cardiovasc Dis* **22**:292-299.
- Barger PM, Brandt JM, Leone TC, Weinheimer CJ and Kelly DP (2000) Deactivation of peroxisome proliferator-activated receptor-alpha during cardiac hypertrophic growth. *J Clin Invest* **105**:1723-1730.
- Bulhak AA, Jung C, Ostenson CG, Lundberg JO, Sjoquist PO and Pernow J (2009) PPAR-alpha activation protects the type 2 diabetic myocardium against ischemia-reperfusion injury: involvement of the PI3-Kinase/Akt and NO pathway. *Am J Physiol Heart Circ Physiol* **296**:H719-727.
- Beatty AL, Zhang MH, Ku IA, Na B, Schiller NB and Whooley MA (2012)

MOL #83964

Adiponectin is associated with increased mortality and heart failure in patients with stable ischemic heart disease: data from the Heart and Soul Study. *Atherosclerosis* **220**:587-592.

Cheng CF, Lian WS, Chen SH, Lai PF, Li HF, Lan YF, Cheng WT and Lin H (2012) Protective effects of adiponectin against renal ischemia-reperfusion injury via prostacyclin-PPARalpha-heme oxygenase-1 signaling pathway. *J Cell Physiol* **227**:239-249.

Chen HH, Chen TW and Lin H (2009) Prostacyclin-induced peroxisome proliferator-activated receptor-alpha translocation attenuates NF-kappaB and TNF-alpha activation after renal ischemia-reperfusion injury. *Am J Physiol Renal Physiol* **297**:F1109-1118.

Crowe S and Bartfay WJ (2002) Amlodipine decreases iron uptake and oxygen free radical production in the heart of chronically iron overloaded mice. *Biol Res Nurs* **3**:189-197.

Finck BN, Lehman JJ, Leone TC, Welch MJ, Bennett MJ, Kovacs A, Han X, Gross RW, Kozak R, Lopaschuk GD, et al. (2002) The cardiac phenotype induced by PPARalpha overexpression mimics that caused by diabetes mellitus. *J Clin Invest* **109**:121-130.

Finck BN, Han X, Courtois M, Aimond F, Nerbonne JM, Kovacs A, Gross RW and

MOL #83964

Kelly DP (2003) A critical role for PPARalpha-mediated lipotoxicity in the pathogenesis of diabetic cardiomyopathy: modulation by dietary fat content.

Proc Natl Acad Sci U S A **100**:1226-1231.

Forouhi NG, Harding AH, Allison M, Sandhu MS, Welch A, Luben R, Bingham S,

Khaw KT and Wareham NJ (2007) Elevated serum ferritin levels predict new-onset type 2 diabetes: results from the EPIC-Norfolk prospective study.

Diabetologia **50**:949-956.

Fraga CG and Oteiza PI (2002) Iron toxicity and antioxidant nutrients. *Toxicology*

180:23-32.

Fujio Y, Nguyen T, Wencker D, Kitsis RN and Walsh K (2002) Akt promotes

survival of cardiomyocytes in vitro and protects against ischemia-reperfusion injury in mouse heart. *Circulation* **101**:660-667.

Gabrielsen JS, Gao Y, Simcox JA, Huang J, Thorup D, Jones D, Cooksey RC,

Gabrielsen D, Adams TD, Hunt SC, et al. (2012) Adipocyte iron regulates adiponectin and insulin sensitivity. *J Clin Invest* **122**:3529-3540.

Genini D and Catapano CV (2006) Control of peroxisome proliferator-activated

receptor fate by the ubiquitin-proteasome system. *J Recept Signal Transduct Res* **26**:679-692.

Gilde AJ, van der Lee KA, Willemsen PH, Chinetti G, van der Leij FR, van der Vusse

MOL #83964

GJ, Staels B and van Bilsen M (2003) Peroxisome proliferator-activated receptor (PPAR) alpha and PPARbeta/delta, but not PPARgamma, modulate the expression of genes involved in cardiac lipid metabolism. *Circ Res* **92**:518-524.

Haemmerle G, Moustafa T, Woelkart G, Buttner S, Schmidt A, van de Weijer T, Hesselink M, Jaeger D, Kienesberger PC, Zierler K, et al. (2011) ATGL-mediated fat catabolism regulates cardiac mitochondrial function via PPAR-alpha and PGC-1. *Nat Med* **17**:1076-1085.

Hajer GR, van Haefen TW and Visseren FL (2008) Adipose tissue dysfunction in obesity, diabetes, and vascular diseases. *Eur Heart J* **29**:2959-2971.

Hopkins TA, Ouchi N, Shibata R and Walsh K (2007) Adiponectin actions in the cardiovascular system. *Cardiovasc Res* **74**:11-18.

Huss JM, Kopp RP and Kelly DP (2002) Peroxisome proliferator-activated receptor coactivator-1alpha (PGC-1alpha) coactivates the cardiac-enriched nuclear receptors estrogen-related receptor-alpha and -gamma. Identification of novel leucine-rich interaction motif within PGC-1alpha. *J Biol Chem* **277**:40265-40274.

Huss JM, Levy FH and Kelly DP (2001) Hypoxia inhibits the peroxisome proliferator-activated receptor alpha/retinoid X receptor gene regulatory

MOL #83964

pathway in cardiac myocytes: a mechanism for O₂-dependent modulation of mitochondrial fatty acid oxidation. *J Biol Chem* **276**:27605-27612.

Huss JM, Torra IP, Staels B, Giguere V and Kelly DP (2004) Estrogen-related receptor alpha directs peroxisome proliferator-activated receptor alpha signaling in the transcriptional control of energy metabolism in cardiac and skeletal muscle. *Mol Cell Biol* **24**:9079-9091.

Kahn E, Baarine M, Pelloux S, Riedinger JM, Frouin F, Tourneur Y and Lizard G (2010) Iron nanoparticles increase 7-ketocholesterol-induced cell death, inflammation, and oxidation on murine cardiac HL1-NB cells. *Int J Nanomedicine* **5**:185-195.

Khan RS, Kato TS, Chokshi A, Chew M, Yu S, Wu C, Singh P, Cheema FH, Takayama H, Harris C, et al. (2012) Adipose tissue inflammation and adiponectin resistance in patients with advanced heart failure: correction after ventricular assist device implantation. *Circ Heart Fail* **5**:340-348.

Konishi M, Haraguchi G, Ohigashi H, Ishihara T, Saito K, Nakano Y and Isobe M (2011) Adiponectin protects against doxorubicin-induced cardiomyopathy by anti-apoptotic effects through AMPK up-regulation. *Cardiovasc Res* **89**:309-319.

Ku BJ, Kim SY, Lee TY and Park KS (2009) Serum ferritin is inversely correlated

with serum adiponectin level: population-based cross-sectional study. *Dis Markers* **27**:303-310.

Kumada M, Kihara S, Sumitsuji S, Kawamoto T, Matsumoto S, Ouchi N, Arita Y, Okamoto Y, Shimomura I, Hiraoka H, et al. (2003) Association of hypoadiponectinemia with coronary artery disease in men. *Arterioscler Thromb Vasc Biol* **23**:85-89.

Lehman JJ, Barger PM, Kovacs A, Saffitz JE, Medeiros DM and Kelly DP (2000) Peroxisome proliferator-activated receptor gamma coactivator-1 promotes cardiac mitochondrial biogenesis. *J Clin Invest* **106**:847-856.

Lian WS, Lin H, Cheng WT, Kikuchi T and Cheng CF (2011) Granulocyte-CSF induced inflammation-associated cardiac thrombosis in iron loading mouse heart and can be attenuated by statin therapy. *J Biomed Sci* **18**:26.

Lin H, Lin TN, Cheung WM, Nian GM, Tseng PH, Chen SF, Chen JJ, Shyue SK, Liou JY, Wu CW, et al. (2002) Cyclooxygenase-1 and bicistronic cyclooxygenase-1/prostacyclin synthase gene transfer protect against ischemic cerebral infarction. *Circulation* **105**:1962-1969.

Lin H, Yu CH, Jen CY, Cheng CF, Chou Y, Chang CC and Juan SH (2010) Adiponectin-mediated heme oxygenase-1 induction protects against iron-induced liver injury via a PPARalpha dependent mechanism. *Am J Pathol*

177:1697-1709.

Maury E and Brichard SM (2010) Adipokine dysregulation, adipose tissue inflammation and metabolic syndrome. *Mol Cell Endocrinol* **314**:1-16.

Mojiminiyi OA, Marouf R and Abdella NA (2008) Body iron stores in relation to the metabolic syndrome, glycemic control and complications in female patients with type 2 diabetes. *Nutr Metab Cardiovasc Dis* **18**:559-566.

Oudit GY, Sun H, Trivieri MG, Koch SE, Dawood F, Ackerley C, Yazdanpanah M, Wilson GJ, Schwartz A, Liu PP, et al. (2003) L-type Ca²⁺ channels provide a major pathway for iron entry into cardiomyocytes in iron-overload cardiomyopathy. *Nat Med* **9**:1187-1194.

Pischon T, Hu FB, Girman CJ, Rifai N, Manson JE, Rexrode KM and Rimm EB (2011) Plasma total and high molecular weight adiponectin levels and risk of coronary heart disease in women. *Atherosclerosis* **219**:322-329.

Rowe GC, Jiang A and Arany Z (2010) PGC-1 coactivators in cardiac development and disease. *Circ Res* **107**:825-838.

Shibata R, Ouchi N, Ito M, Kihara S, Shiojima I, Pimentel DR, Kumada M, Sato K, Schiekofer S, Ohashi K, et al. (2004) Adiponectin-mediated modulation of hypertrophic signals in the heart. *Nat Med* **10**:1384-1389.

Shibata R, Sato K, Pimentel DR, Takemura Y, Kihara S, Ohashi K, Funahashi T,

MOL #83964

- Ouchi N and Walsh K (2005) Adiponectin protects against myocardial ischemia-reperfusion injury through AMPK- and COX-2-dependent mechanisms. *Nat Med* **11**:1096-1103.
- Springer J, Anker SD and Doehner W (2010) Adiponectin resistance in heart failure and the emerging pattern of metabolic failure in chronic heart failure. *Circ Heart Fail* **3**:181-182.
- Tian L, Luo N, Zhu X, Chung BH, Garvey WT and Fu Y (2012) Adiponectin-AdipoR1/2-APPL1 signaling axis suppresses human foam cell formation: differential ability of AdipoR1 and AdipoR2 to regulate inflammatory cytokine responses. *Atherosclerosis* **221**:66-75.
- Vaiopoulos AG, Marinou K, Christodoulides C and Koutsilieris M (2012) The role of adiponectin in human vascular physiology. *Int J Cardiol* **155**:188-193.
- Wang Z, Zhu T, Qiao C, Zhou L, Wang B, Zhang J, Chen C, Li J, Xiao X (2005) Adeno-associated virus serotype 8 efficiently delivers genes to muscle and heart. *Nat Biotechnol* **23**:321-328.
- Wang Y, Lau WB, Gao E, Tao L, Yuan Y, Li R, Wang X, Koch WJ and Ma XL (2010) Cardiomyocyte-derived adiponectin is biologically active in protecting against myocardial ischemia-reperfusion injury. *Am J Physiol Endocrinol Metab* **298**:E663-670.

MOL #83964

Won H, Kang SM, Shin MJ, Oh J, Hong N, Park S, Lee SH, Jang Y and Chung N

(2012) Plasma adiponectin concentration and its association with metabolic syndrome in patients with heart failure. *Yonsei Med J* **53**:91-98.

Zhu W, Cheng KK, Vanhoutte PM, Lam KS and Xu A (2008) Vascular effects of

adiponectin: molecular mechanisms and potential therapeutic intervention.

Clin Sci (Lond) **114**:361-374.

Zoccali C, Mallamaci F, Tripepi G, Benedetto FA, Cutrupi S, Parlongo S, Malatino

LS, Bonanno G, Seminara G, Rapisarda F, et al. (2002) Adiponectin,

metabolic risk factors, and cardiovascular events among patients with

end-stage renal disease. *J Am Soc Nephrol* **13**:134-141.

MOL #83964

Footnotes

H.L. and W.-S.L. contributed equally to this work.

Financial support: This work is supported by the grants from Tzu Chi Hospital [TCDR101-10, TCRDI-100-01-03], Tzu Chi University [TCIRP 99001], and National Science Council [98-2314-B-303-001-MY3] to Ching-Feng Cheng.

Conflict of interest: none declared

Figure legends

Fig. 1. Survival rate and serum adiponectin concentrations in mice after iron loading for four weeks. (A) Cumulative survival rate after iron loading to mice for 4 weeks. Iron dextran was given to mice (10 mg/ 25 gm body weight/day, i.p.) 5 times /week for total 4 weeks periods. Kaplan-Meier survival curves showed decreased survival in iron treatment group compared with the control group injected with same volume of saline over 4 weeks period. (B) Serum adiponectin levels in mice after iron treatment for 4 weeks. * $p < 0.05$, compared with the control group (C).

Fig. 2. In vivo AAV8-ADIPOQ therapy attenuated iron deposition in mice heart.

ADIPOQ (AAV8-ADIPOQ; 1×10^{12} particles / mouse) or AAV8-CMV as control, were mixed with cardiac lysates for i.v. injection. (A and B) The cardiac expression of adiponectin (APN) in different dosages were analyzed by western blotting 2 weeks after ADIPOQ over-expressed in heart (A), and the cardioprotective effects of AAV8-ADIPOQ as compared with other organs were demonstrated using qPCR analysis (B). (C) The serum concentration of adiponectin after AAV8-ADIPOQ treatment, assayed by ELISA (n=7). Data were repeated for three times with similar results. (D) Representative photographs of left ventricular histology in iron-overload mice with or without AAV8-ADIPOQ treatment. Heart sections were stained with

MOL #83964

iron staining; n = 7 in each group; * $p < 0.05$.

Fig. 3. ADIPOQ overexpression restored normal left ventricular contraction and

ameliorated cardiac inflammation in iron-loading mice. (A) Parameters on

echocardiographic results were demonstrated in mice after 4 weeks of iron-loading

with or without AAV8-ADIPOQ therapy, including heart rates ((HR); left ventricular

fraction shortening (FS) and ejection fraction (EF); thickness of inter-ventricular

septum at diastole (IVSd) and systole (IVSs); and left ventricular internal diameter at

diastole (LVIDd) and systole (LVIDs). Values are mean \pm SEM (n=5 per group);

* $p < 0.05$. (B) MPO (myelo-peroxidase) activity of cardiac tissue in iron-loading mice

with or without ADIPOQ therapy. MPO activity is expressed as the absorbance at 460

nm/min per mg protein (n = 8 mice in each group). * $p < 0.05$. (C) ELISA analysis of

MCP-1, IL-6, ICAM-1, and TNF α level from sera derived from iron-loading mice

with or without ADIPOQ therapy. (D) Quantitative RT-PCR analysis of TNF α and

ICAM-1 level from heart cDNA derived from iron-loading mice with or without

ADIPOQ therapy. Expression levels were normalized to those of GAPDH. Values are

mean \pm SEM (n = 6 mice in each group).

Fig. 4. Adiponectin (APN) mediated HO-1 expression via AMPK-PPAR α

pathway in cardiomyocytes. (A) Protein levels of AMPK and p-AMPK in H9c2 cells under APN supplement (5 or 50 μ g) for 24 hours (left panel). Protein levels of AMPK, p-AMPK, and HO-1 in H9c2 cells under APN protein (50 μ g) supplement for 0.5, 1, 3, or 6 hours, respectively (right panel). (B) APN induced HO-1 expression in a time dependent manners. Rat neonatal cardiomyocytes were infected with 100 moi adenovirus (Adv) containing ADIPOQ or HPGK (as control) for 12, 18, or 24 hours, respectively. Data were acquired from three independent experiments with similar results. (C) Western blotting analysis of PPAR α in cytosolic and nuclear fractions of neonatal cardiomyocytes after infection with adenovirus (Adv) containing ADIPOQ or HPGK (as control) for 18 or 24 hours, respectively. (D) CHIP assay. Chromatin was isolated from APN protein-treated or untreated H9c2 cells for 0.5, 1, 3 or 6 hours, respectively. PPAR α specific antibodies and primers to amplify HO-1 promoters locus (-1421 to -1400) which contained one predicted PPAR α -response element (PPRE), were used. Immunoprecipitated DNA was then assayed by PCR. (E) Over-expression of ADIPOQ by adenovirus containing ADIPOQ induced PPRE-luciferase activity. H9c2 cells were transiently transfected using luciferase vector (pGL2) with HO-1 promoter containing PPRE-binding site, and infected with 50 or 100 moi adenovirus containing ADIPOQ or HPGK, respectively. Cells were collected and assayed for luciferase activity; * p <0.05. (F) Exogenous APN therapy

MOL #83964

induced PPRE-leuciferase activity. H9c2 cells, transiently transfected with reporter constructs pGL2-PPRE, were treated with 2 concentrations (10 or 20 μg , respectively) of APN purified from *E. coli*; then cells were collected and assayed for luciferase activity; $*p < 0.05$.

Fig 5. ADIPOQ mediated beneficial effects in iron-overload cardiomyopathy were PPAR α dependent. Representative photographs of left ventricular histology in PPAR α knock out (ko) or their wild type (WT) littermate mice after 4 weeks of iron loading with or without AAV8-ADIPOQ therapy. Paraformaldehyde-fixed sections were stained with iron staining. (n=5 in each group). Each histogram represents the number of iron positively-stained cells in each group; Bar = 200 μm . $*p < 0.05$.

Fig. 6. Adiponectin (APN) enhanced PPAR α expression and nuclear translocation in association with PGC-1. (A) Expression of PPAR α and PGC-1 protein levels in the cytosolic (left upper panel) and nuclear (left lower panel) fractions of the H9c2 cell lines after iron treatment for 24 hours. (B) APN supplement enhanced nuclear translocation of PPAR α and PGC-1. Cell lysates from iron loaded H9c2 cells were treated with or without APN (50 μg) and then separated into nuclear and cytosolic fractions, respectively; and probed with specific antibody against

MOL #83964

PPAR α or PGC-1. Representative results were acquired from two independent experiments. (C) APN can increase PPAR α and PGC-1 binding in iron treated H9c2 cells. H9c2 cells were treated with iron (10 or 20 μ M, respectively) and supplied with or without APN for 24 hours, then whole cells lysis were collected for immuno-precipitated with anti-PPAR α or anti-PGC-1 antibody followed by immune-blotting with individual antibody. The anti-actin immune-blotting was served as sample control. Scanning densitometries in (A), (B), and (C) were used for semi-quantitative analysis in compared to the actin or lamin A/C levels, respectively (right panel); * p < 0.05.

Table 1. Blood count parameters (mean \pm SD) acquired at end of fourth weeks in iron-loading mice with or without AAV-ADIPOQ treatment

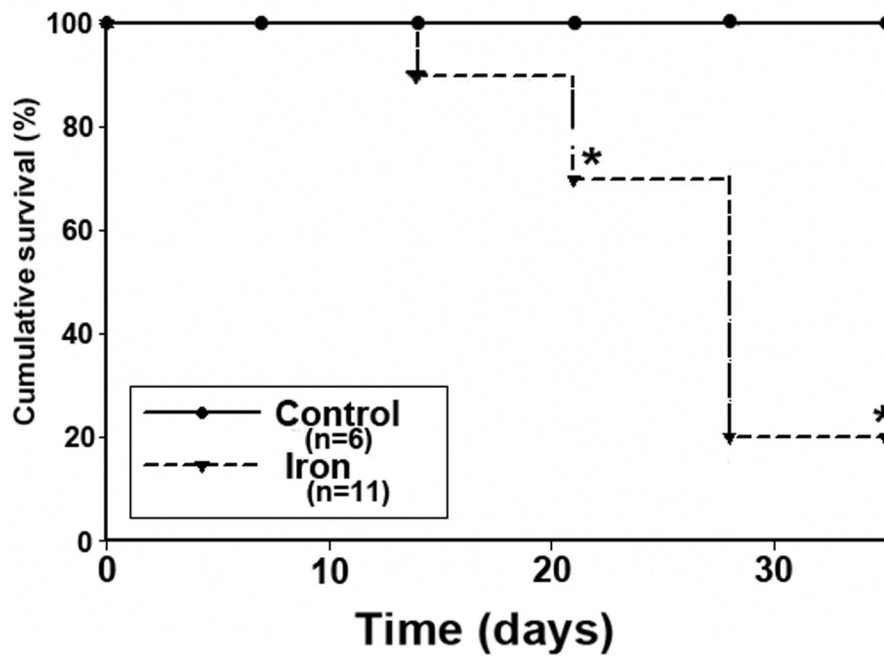
	LEUK ($10^9/L$)	ERY ($10^{12}/L$)	HGB (g/dl)	NEU ($10^9/L$)	LYM ($10^9/L$)	MONO ($10^9/L$)	PLT ($10^9/L$)
C	8.9 \pm 1.64	9.04 \pm 0.27	16.08 \pm 0.77	1.75 \pm 0.18	6.46 \pm 1.47	0.19 \pm 0.02	1514.4 \pm 76.52
I	26.67 \pm 1.94*	8.26 \pm 0.27	15.46 \pm 0.32	11.35 \pm 0.22**	9.82 \pm 1.47*	2.26 \pm 0.32*	1313.8 \pm 134.5
I+ADIPOQ	20.93 \pm 2.81 [†]	7.04 \pm 2.05	14.96 \pm 0.69	11.21 \pm 2.97	7.45 \pm 1.56 [†]	2.25 \pm 0.77	1281.4 \pm 119.63

LEUK, leukocytes; ERY, erythrocytes; HGB, hemoglobin; NEU, neutrophil; LYM, lymphocyte; MONO, monocyte; PLT, platelet; * $p < 0.05$, ** $p < 0.01$ v.s. control group (C); [†] $p < 0.05$ v.s. iron-overload group (I), $n = 6\sim 8$ in each group.

Fig. 1

Molecular Pharmacology Fast Forward. Published on May 30, 2013 as DOI: 10.1124/mol.112.083964
This article has not been copyedited and formatted. The final version may differ from this version.

(A)



(B)

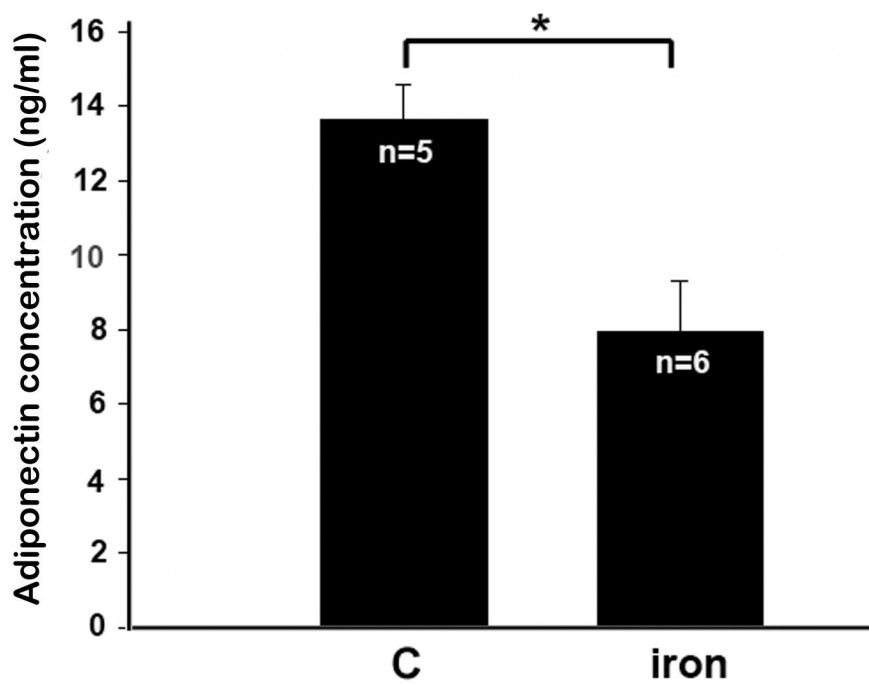
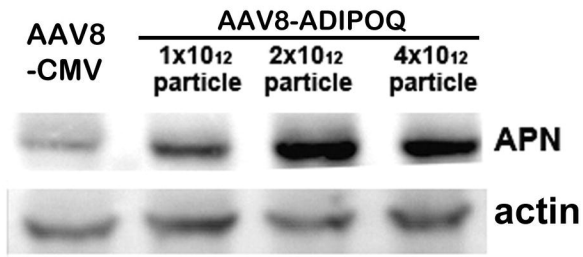


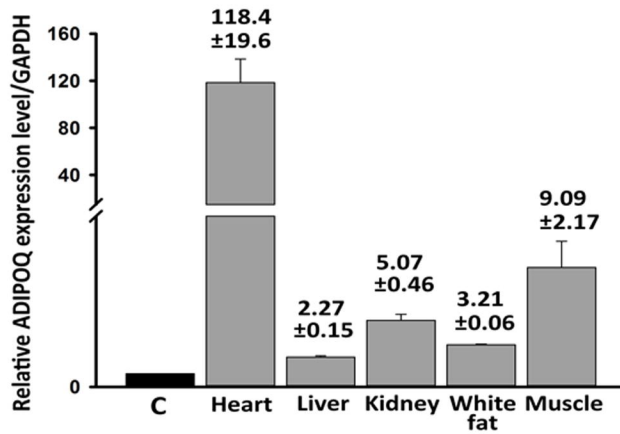
Fig. 2

Molecular Pharmacology Fast Forward. Published on May 30, 2013 as DOI: 10.1124/mol.112.083964
This article has not been copyedited and formatted. The final version may differ from this version.

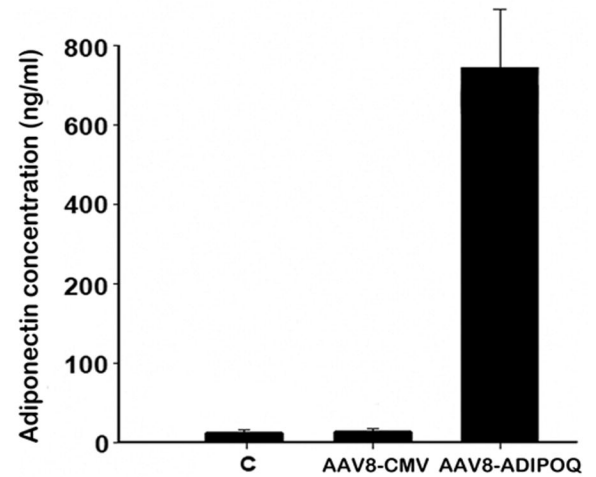
(A)



(B)



(C)



(D)

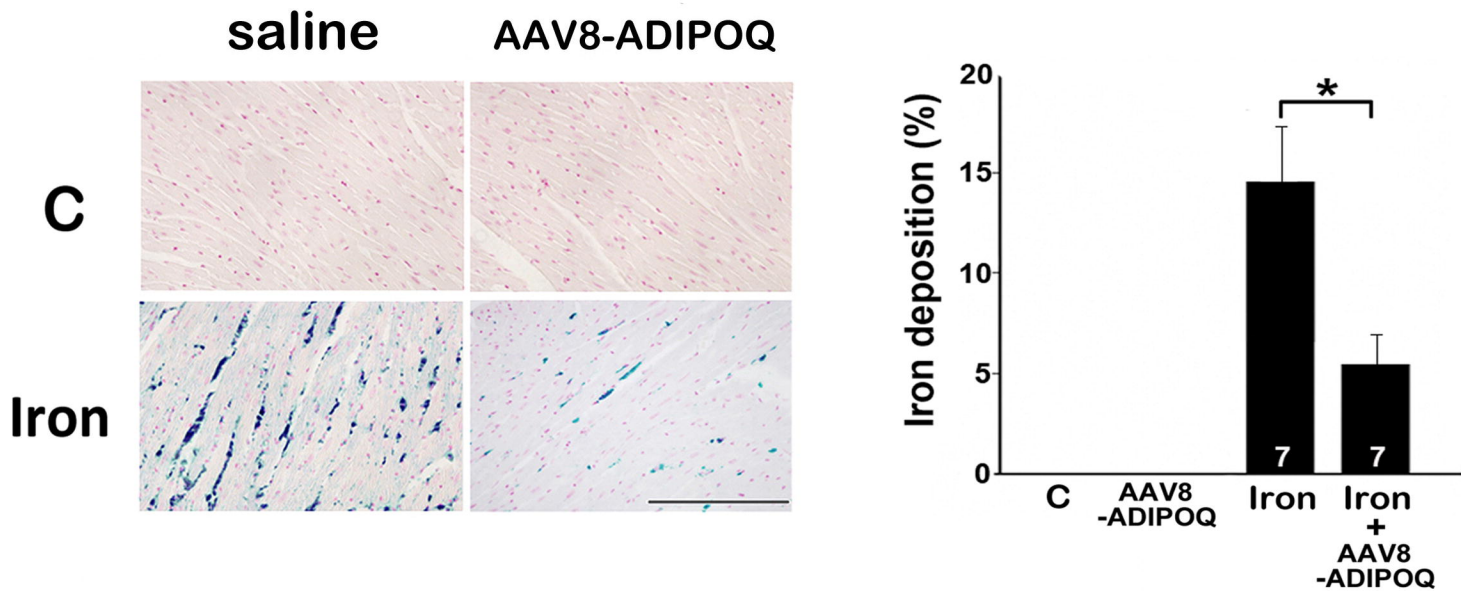
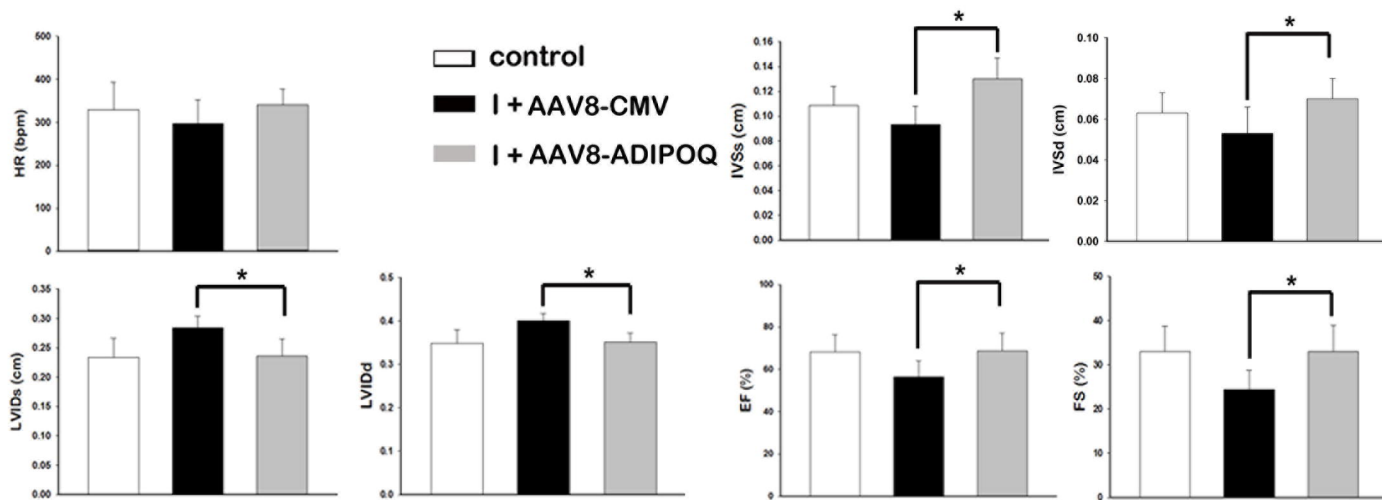


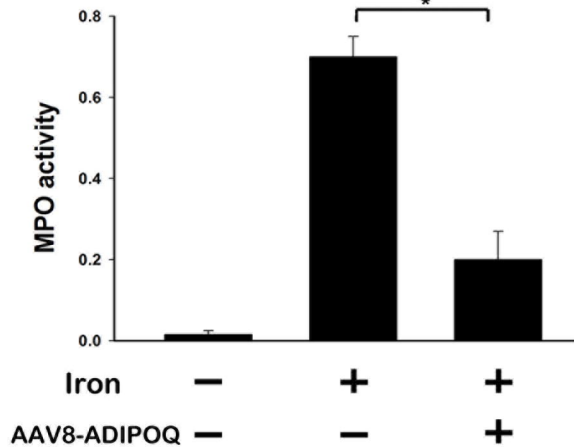
Fig. 3

Molecular Pharmacology Fast Forward. Published on May 30, 2013 as DOI: 10.1124/mol.112.083964
 This article has not been copyedited and formatted. The final version may differ from this version.

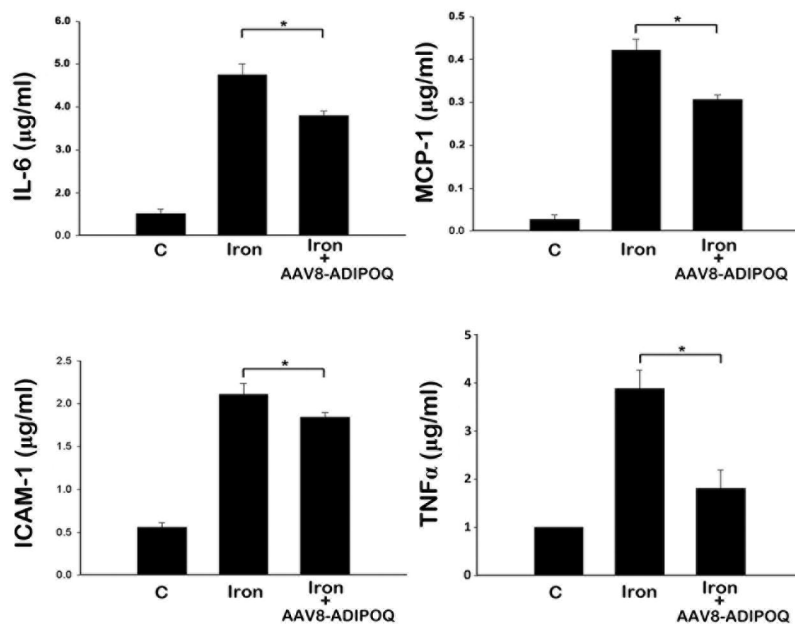
(A)



(B)



(C)



(D)

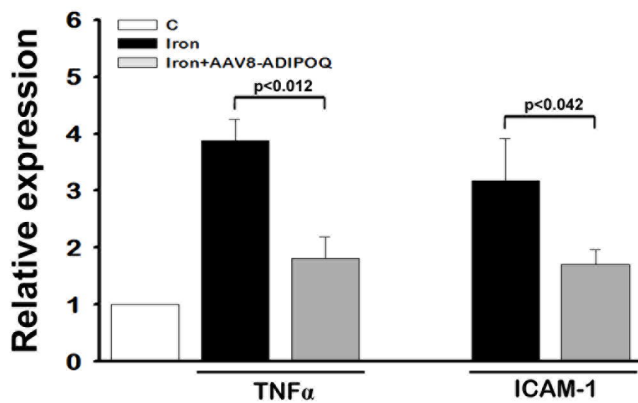


Fig. 4

Molecular Pharmacology Fast Forward. Published on May 30, 2013 as DOI: 10.1124/mol.112.083964
 This article has not been copyedited and formatted. The final version may differ from this version.

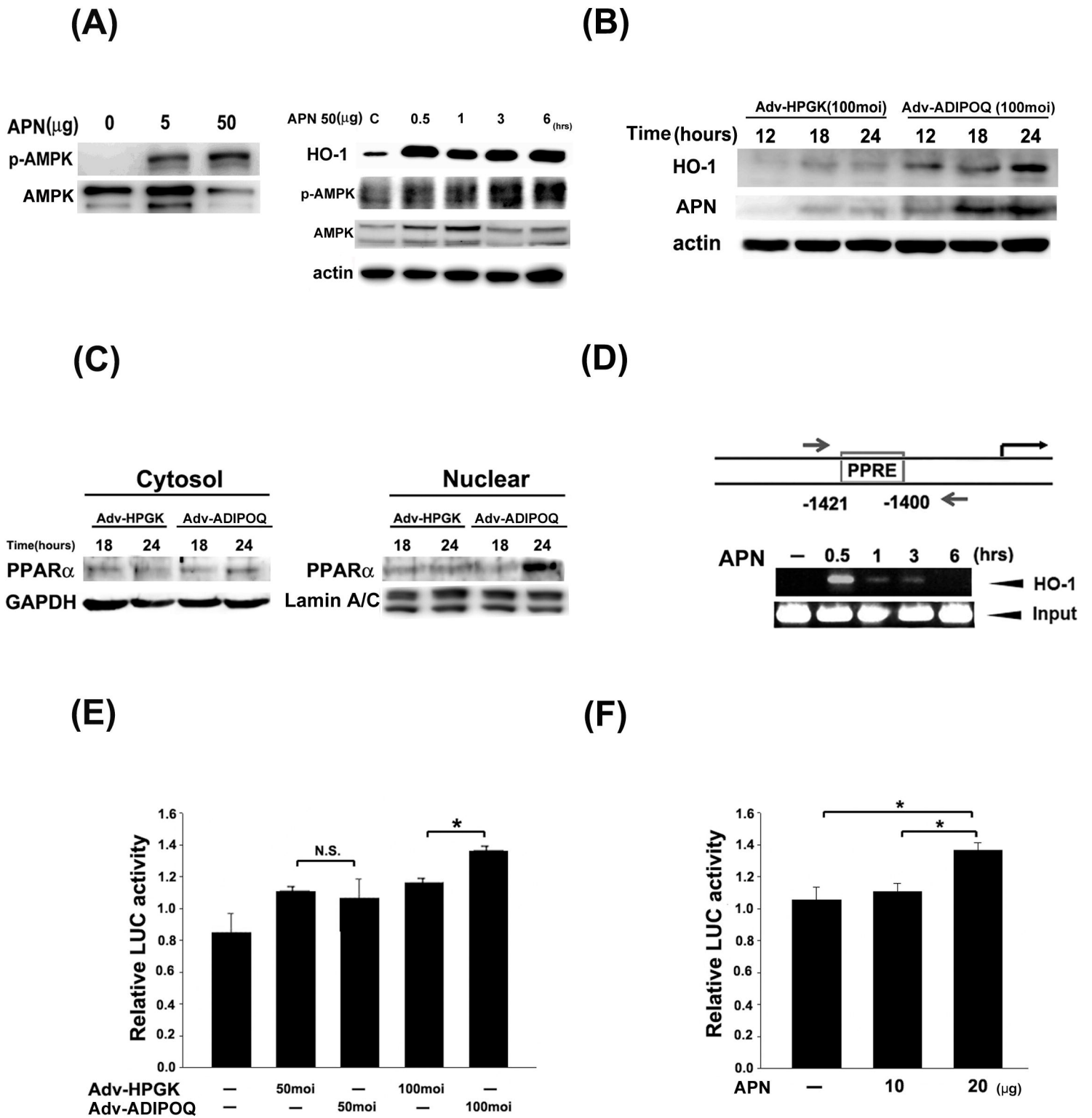


Fig. 5

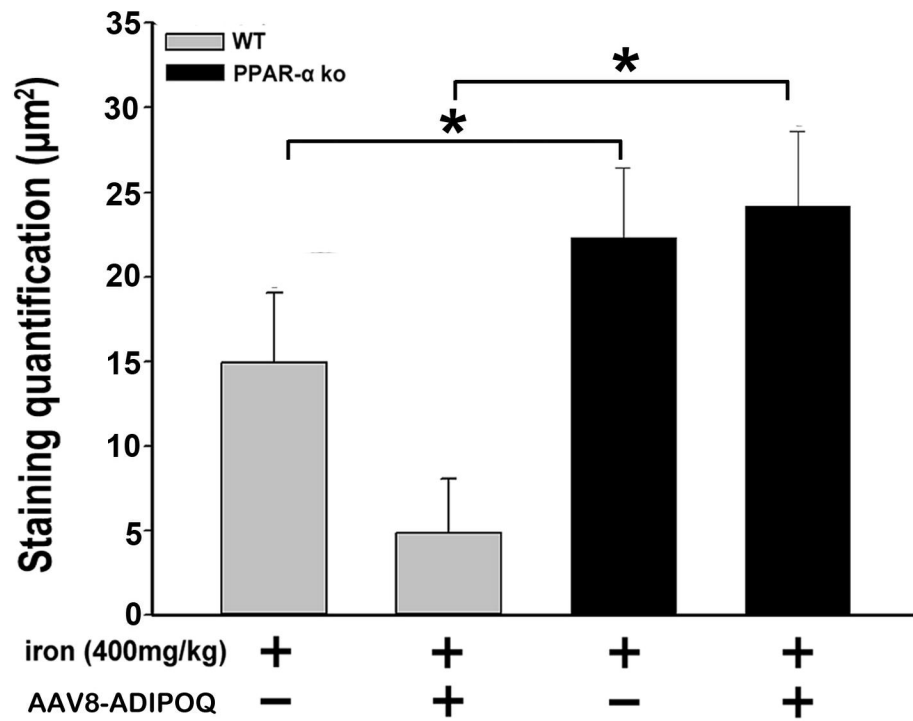
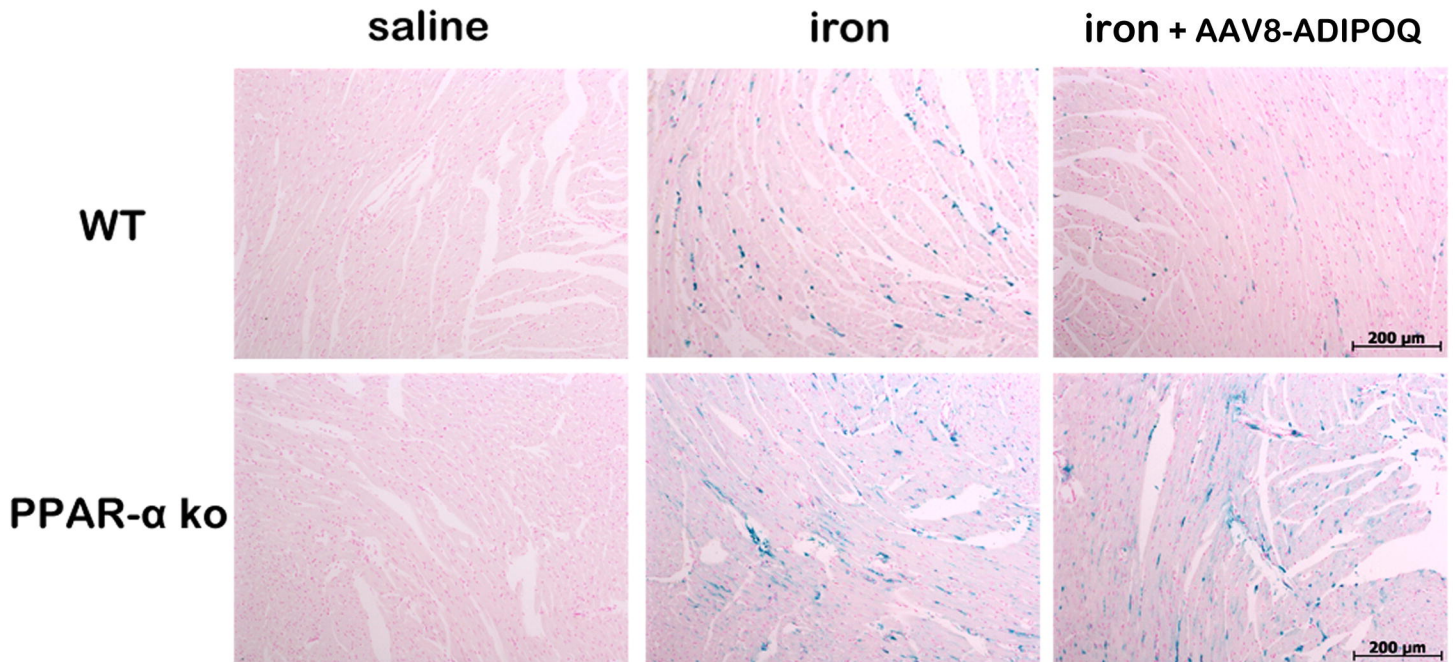
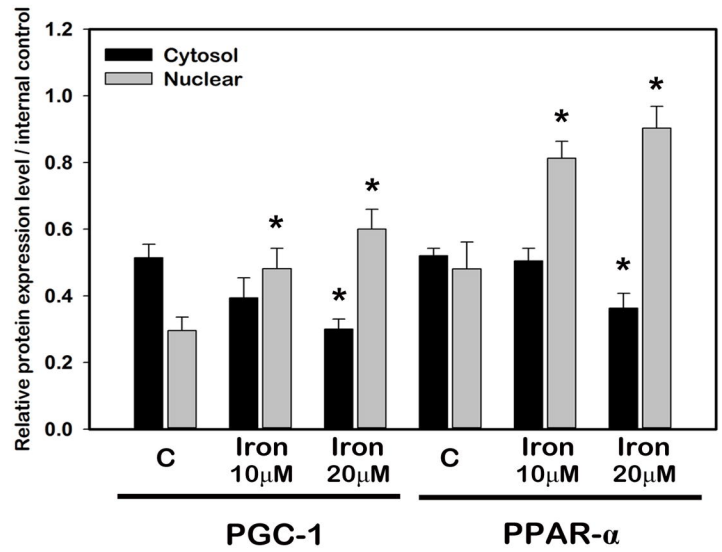
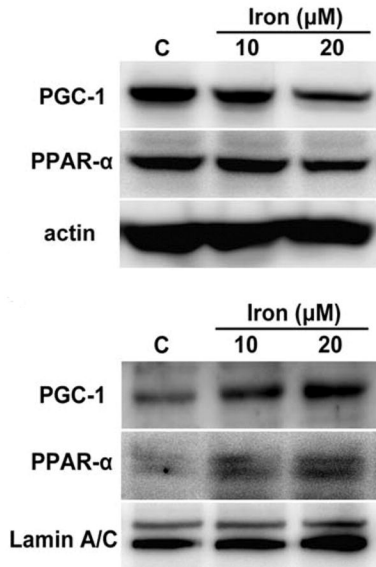


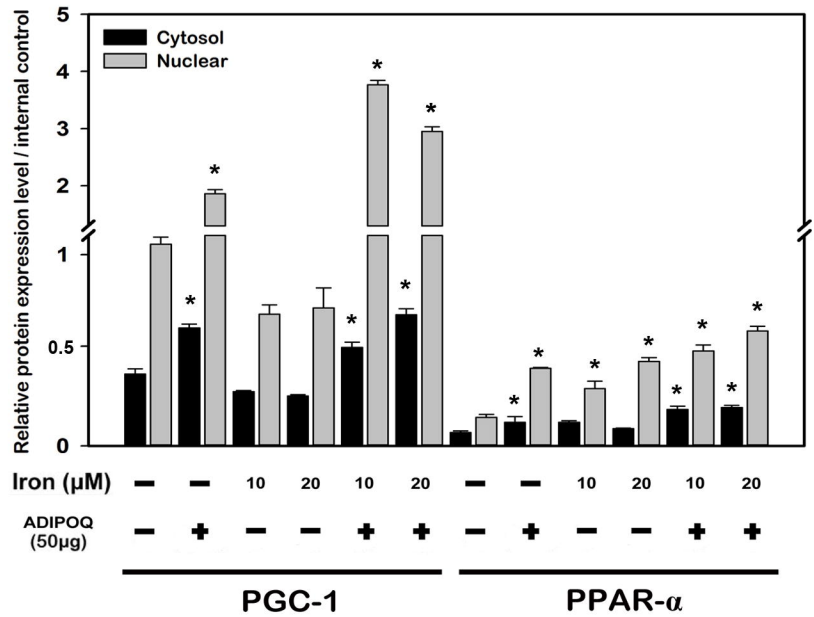
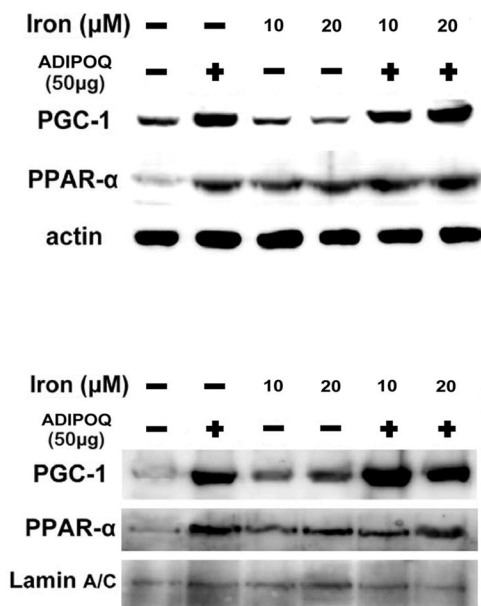
Fig. 6

Molecular Pharmacology Fast Forward. Published on May 30, 2013 as DOI: 10.1124/mol.112.083964
 This article has not been copyedited and formatted. The final version may differ from this version.

(A)



(B)



(C)

